

Critical study of the $B \rightarrow K\pi$ puzzleC. S. Kim,^{1,2,*} Sechul Oh,^{3,†} and Chaehyun Yu^{1,‡}¹*Department of Physics, Yonsei University, Seoul 120-479, Korea*²*Graduate School of Science, Hiroshima University, Higashi-Hiroshima, Japan 739-8536*³*Natural Science Research Institute, Yonsei University, Seoul 120-479, Korea*

(Received 9 May 2005; revised manuscript received 4 August 2005; published 7 October 2005)

In the light of new experimental results on $B \rightarrow K\pi$ decays, we critically study the decay processes $B \rightarrow K\pi$ in a phenomenological way. Using the quark diagram approach and the currently available data, we determine the allowed values of the relevant theoretical parameters, corresponding to the electroweak (EW) penguin, the color-suppressed tree contribution, etc. In order to find the most likely values of the parameters in a statistically reliable way, we use the χ^2 minimization technique. Our result shows that the current data for $B \rightarrow K\pi$ decays strongly indicate (large) enhancements of both the EW penguin and the color-suppressed tree contributions. In particular, the color-suppressed tree effect needs to be enhanced by about an order of magnitude to fit the present data.

DOI: [10.1103/PhysRevD.72.074005](https://doi.org/10.1103/PhysRevD.72.074005)

PACS numbers: 13.25.Hw

I. INTRODUCTION

From B factory experiments such as Belle and BABAR, a tremendous amount of experimental data on B meson decays are being collected and provide new limits on previously known observables with great precision as well as an opportunity to see very rare processes for the first time. Experimentally plenty of two-body hadronic B decays have been observed and some of data for these decay modes, such as $B \rightarrow K\pi$, are now quite precise, which leads to a precision era for the study of two-body hadronic B decays.

There are four different decay channels (and their anti-particle decay channels) for $B \rightarrow K\pi$ processes, depending on the electric charge configuration: $B^+ \rightarrow K^0\pi^+$, $B^+ \rightarrow K^+\pi^0$, $B^0 \rightarrow K^+\pi^-$, and $B^0 \rightarrow K^0\pi^0$. All the $B \rightarrow K\pi$ modes have already been observed in experiment and their CP -averaged branching ratios have been measured within a few percent errors by the BABAR and Belle collaborations [1–7]. The measurements of direct CP asymmetries for the $B \rightarrow K\pi$ modes had contained large errors so that the results have not led to any decisive conclusions until recently [1,8–13]. But, the observations of the direct CP asymmetry in $B^0 \rightarrow K^\pm\pi^\mp$ have been recently achieved at the 5.7σ level by BABAR and Belle [10–12]. For the other $B \rightarrow K\pi$ modes, the experimental results of the direct CP asymmetries still include large errors. Certain experimental data (e.g., the branching ratios (BRs)) for $B \rightarrow K\pi$ are currently more precise than the theoretical model predictions based on QCD factorization, perturbative QCD (pQCD), and so on. Thus, these decay modes can provide very useful information for improving the model calculations. Therefore, at the same time, the model-independent study becomes very important.

In the light of those new data, including the direct CP asymmetry in $B^0 \rightarrow K^\pm\pi^\mp$, many works have been recently done to study the implications of the data [14–22]. The quark level subprocesses for $B \rightarrow K\pi$ decays are $b \rightarrow sq\bar{q}$ ($q = u, d$) penguin processes which are potentially sensitive to any new physics effects beyond the standard model (SM). Thus, with the currently available precision data, it is very important to investigate these modes as generally and critically as possible. In this work, we critically study the decay processes $B \rightarrow K\pi$ in a phenomenological way. In particular, by noticing that the current data for $B \rightarrow K\pi$ can be divided into two groups (relatively precise ones and the other ones), to be conservative, we try to investigate the implications of the current experimental results systematically in a few steps, as we shall see later. We are mainly interested in investigating whether the conventional SM predictions are consistent with the current data. Furthermore, if there are some deviations between the conventional estimates and the experimental results, we intend to carefully identify the source of the deviations and estimate how large the contribution from the source can be. For this aim, we use the topological amplitudes in the quark diagram approach and try to determine the allowed values of the relevant theoretical parameters, corresponding to the electroweak (EW) penguin, the color-suppressed tree contribution, and so on, by the current data. We should emphasize that the parameter values determined in this way are model-independent. Then, by comparing our result with the conventional SM predictions, we shall be able to verify whether the current data indicate any new physics effects. In order to find the most likely values of the theoretical parameters in a statistically reliable way, we will adopt the χ^2 analysis. In this work, we do not consider $B \rightarrow \pi\pi$ modes simultaneously with $B \rightarrow K\pi$ modes, though they can be connected to each other by using flavor SU(3) symmetry. It is because we do not want that our analysis would be spoiled by the unknown effects of the flavor SU(3) breaking. Also, as it

*Email address: cskim@yonsei.ac.kr

†Email address: scoh@phya.yonsei.ac.kr

‡Email address: chyuu@cskim.yonsei.ac.kr

turns out, the data on $B \rightarrow K\pi$ provide enough information for the analysis.

The paper is organized as follows. The relevant formulas for $B \rightarrow K\pi$ modes are presented in Sec. II. In Sec. III, the experimental results for $B \rightarrow K\pi$ are summarized and their implications are investigated. In Sec. IV, the χ^2 analysis using $B \rightarrow K\pi$ decays is presented. We conclude the analysis in Sec. V.

II. THE RELEVANT FORMULAS FOR $B \rightarrow K\pi$ DECAY MODES

In order to specify our notation, let us first summarize the formulas for the relevant decay amplitudes, BRs, direct and indirect (mixing-induced) CP asymmetries. The decay amplitudes for two-body hadronic B decays can be represented in terms of the basis of topological quark diagram contributions [23]. The relevant decay amplitudes for $B \rightarrow K\pi$ can be written as [24]

$$A^{0+} \equiv A(B^+ \rightarrow K^0 \pi^+) = V_{ub}^* V_{us} \tilde{A} + V_{tb}^* V_{ts} \tilde{P}, \quad (1)$$

$$A^{+0} \equiv A(B^+ \rightarrow K^+ \pi^0) = -\frac{1}{\sqrt{2}} [V_{ub}^* V_{us} (\tilde{T} + \tilde{C} + \tilde{A}) + V_{tb}^* V_{ts} (\tilde{P} + \tilde{P}_{EW} + \tilde{P}_{EW}^C)], \quad (2)$$

$$A^{+-} \equiv A(B^0 \rightarrow K^+ \pi^-) = -[V_{ub}^* V_{us} \tilde{T} + V_{tb}^* V_{ts} (\tilde{P} + \tilde{P}_{EW}^C)], \quad (3)$$

$$A^{00} \equiv A(B^0 \rightarrow K^0 \pi^0) = -\frac{1}{\sqrt{2}} [V_{ub}^* V_{us} \tilde{C} - V_{tb}^* V_{ts} (\tilde{P} - \tilde{P}_{EW})], \quad (4)$$

where V_{ij} ($i = u, t; j = s, b$) are Cabibbo-Kobayashi-Maskawa (CKM) matrix elements and the amplitudes \tilde{T} , \tilde{C} , \tilde{A} , \tilde{P} , \tilde{P}_{EW} , and \tilde{P}_{EW}^C are defined as

$$\tilde{T} \equiv T + P_u + E_u - P_c - E_c, \quad (5)$$

$$\tilde{C} \equiv C - P_u - E_u + P_c + E_c, \quad (6)$$

$$\tilde{A} \equiv A + P_u + E_u - P_c - E_c, \quad (7)$$

$$\tilde{P} \equiv P_t + E_t - P_c - E_c - \frac{1}{3} P_{EW}^C + \frac{2}{3} E_{EW}^C, \quad (8)$$

$$\tilde{P}_{EW} \equiv P_{EW} + E_{EW}^C, \quad (9)$$

$$\tilde{P}_{EW}^C \equiv P_{EW}^C - E_{EW}^C. \quad (10)$$

Here T is a color-favored tree amplitude, C is a color-suppressed tree, A is an annihilation, P_i ($i = u, c, t$) is a QCD penguin, E_i is a penguin exchange, P_{EW} is a color-favored EW penguin, P_{EW}^C is a color-suppressed EW pen-

guin, E_{EW}^C is a color-suppressed EW penguin exchange diagram.

Since the QCD penguin contribution is dominant in $B \rightarrow K\pi$ decays, the decay amplitudes are rewritten as [24]

$$A^{0+} = -|V_{tb}^* V_{ts}| \tilde{P} [1 - r_A e^{i\delta^A} e^{i\phi_3}], \quad (11)$$

$$A^{+0} = \frac{1}{\sqrt{2}} |V_{tb}^* V_{ts}| \tilde{P} [1 - (r_T e^{i\delta^T} + r_C e^{i\delta^C} + r_A e^{i\delta^A}) e^{i\phi_3} + r_{EW} e^{i\delta^{EW}} + r_{EW}^C e^{i\delta^{EWC}}], \quad (12)$$

$$A^{+-} = |V_{tb}^* V_{ts}| \tilde{P} [1 - r_T e^{i\delta^T} e^{i\phi_3} + r_{EW}^C e^{i\delta^{EWC}}], \quad (13)$$

$$A^{00} = -\frac{1}{\sqrt{2}} |V_{tb}^* V_{ts}| \tilde{P} [1 - r_{EW} e^{i\delta^{EW}} + r_C e^{i\delta^C} e^{i\phi_3}], \quad (14)$$

where the ratios of each contribution to the dominant one are defined as

$$r_A = \frac{|V_{ub}^* V_{us} \tilde{A}|}{|V_{tb}^* V_{ts} \tilde{P}|}, \quad r_T = \frac{|V_{ub}^* V_{us} \tilde{T}|}{|V_{tb}^* V_{ts} \tilde{P}|}, \quad (15)$$

$$r_C = \frac{|V_{ub}^* V_{us} \tilde{C}|}{|V_{tb}^* V_{ts} \tilde{P}|},$$

$$r_{EW} = \frac{|\tilde{P}_{EW}|}{|\tilde{P}|}, \quad r_{EW}^C = \frac{|\tilde{P}_{EW}^C|}{|\tilde{P}|}. \quad (16)$$

Here δ^X denotes the relative strong phase between each amplitude \tilde{X} and the dominant \tilde{P} , and ϕ_3 ($\equiv \gamma$) is the angle of the unitarity triangle. We note that there exists a conventional hierarchy among the above ratios:

$$1 > r_T \sim r_{EW} > r_C \sim r_{EW}^C > r_A. \quad (17)$$

For instance, in the pQCD approach, those ratios are roughly estimated as [14,25]

$$r_T \approx 0.21, \quad r_{EW} \approx 0.14, \quad r_C \approx 0.02, \\ r_{EW}^C \approx 0.01, \quad r_A \approx 0.005. \quad (18)$$

It is also known that within the SM, under flavor SU(3) symmetry, the relation $\delta^T \approx \delta^{EW}$ holds to a good approximation [26], which can be deduced from the fact that the topology of the color-allowed tree diagram is similar to that of the EW penguin diagram.

Then the CP -averaged BRs are given by

$$\bar{B}^{0+} \equiv \bar{B}(B^\pm \rightarrow K\pi^\pm) \propto \frac{1}{2} [|A^{0+}|^2 + |A^{0-}|^2] \\ = |V_{tb}^* V_{ts}|^2 |\tilde{P}|^2 [1 - 2r_A \cos\delta^A \cos\phi_3], \quad (19)$$

$$\begin{aligned}
2\bar{\mathcal{B}}^{+0} &\equiv 2\bar{\mathcal{B}}(B^\pm \rightarrow K^\pm \pi^0) \propto [|A^{+0}|^2 + |A^{-0}|^2] \\
&= |V_{ib}^* V_{is}|^2 |\tilde{P}|^2 \{1 + 2r_{EW} \cos \delta^{EW} + 2r_{EW}^C \cos \delta^{EW} \\
&\quad - 2(r_T \cos \delta^T + r_C \cos \delta^C + r_A \cos \delta^A) \cos \phi_3 \\
&\quad + r_T^2 + r_{EW}^2 + r_C^2 - 2[r_T r_{EW} \cos(\delta^T - \delta^{EW}) \\
&\quad + r_C r_{EW} \cos(\delta^C - \delta^{EW}) - r_T r_C \cos(\delta^T - \delta^C)] \\
&\quad \times \cos \phi_3\}, \quad (20)
\end{aligned}$$

$$\begin{aligned}
\bar{\mathcal{B}}^{+-} &\equiv \bar{\mathcal{B}}(B_d \rightarrow K^\pm \pi^\mp) \propto \frac{1}{2} [|A^{+-}|^2 + |A^{-+}|^2] \\
&= |V_{ib}^* V_{is}|^2 |\tilde{P}|^2 [1 - 2r_T \cos \delta^T \cos \phi_3 \\
&\quad + 2r_{EW}^C \cos \delta^{EW} + r_T^2], \quad (21)
\end{aligned}$$

$$\begin{aligned}
2\bar{\mathcal{B}}^{00} &\equiv 2\bar{\mathcal{B}}(B_d \rightarrow K \pi^0) \propto [|A^{00}|^2 + |A^{00}|^2] \\
&= |V_{ib}^* V_{is}|^2 |\tilde{P}|^2 [1 - 2r_{EW} \cos \delta^{EW} \\
&\quad + 2r_C \cos \delta^C \cos \phi_3 + r_{EW}^2 + r_C^2] \\
&\quad - 2r_{EW} r_C \cos(\delta^{EW} - \delta^C) \cos \phi_3. \quad (22)
\end{aligned}$$

Here we neglect the r^2 terms which include tiny quantities r_A and r_{EW}^C . However, because recent studies on two-body hadronic B decays show that the color-suppressed tree contribution could be enhanced to a large amount through certain mechanisms [27–29], we keep the r^2 terms including r_C , in order to take that possibility into account. This treatment differs from that in Refs. [14,24], where all the r^2 terms including r_A and r_{EW}^C as well as r_C were simply neglected. In fact, we shall see that a large enhancement of the color-suppressed tree contribution is indicated by the present experimental data for $B \rightarrow K\pi$ modes.

The ratios between the BRs for the $B \rightarrow K\pi$ modes can be also defined as

$$R_1 = \frac{\tau^+ \bar{\mathcal{B}}^{+-}}{\tau^0 \bar{\mathcal{B}}^{0+}} = 1 - 2r_T \cos \delta^T \cos \phi_3 + r_T^2, \quad (23)$$

$$\begin{aligned}
R_c &= \frac{2\bar{\mathcal{B}}^{+0}}{\bar{\mathcal{B}}^{0+}} = 1 + 2r_{EW} \cos \delta^{EW} - 2(r_T \cos \delta^T + r_C \cos \delta^C) \\
&\quad \times \cos \phi_3 + r_T^2 + r_{EW}^2 + r_C^2 + 2r_T r_C \cos(\delta^T - \delta^C) \\
&\quad - 2[r_{EW} r_T \cos(\delta^{EW} - \delta^T) \\
&\quad + r_{EW} r_C \cos(\delta^{EW} - \delta^C)] \cos \phi_3, \quad (24)
\end{aligned}$$

$$\begin{aligned}
R_n &= \frac{\bar{\mathcal{B}}^{+-}}{2\bar{\mathcal{B}}^{00}} = 1 + 2r_{EW} \cos \delta^{EW} - 2(r_T \cos \delta^T + r_C \cos \delta^C) \\
&\quad \times \cos \phi_3 + r_T^2 - r_{EW}^2 - r_C^2 + 4r_{EW}^2 \cos^2 \delta^{EW} \\
&\quad + 2r_{EW} [r_C \cos(\delta^{EW} - \delta^C) - 2r_T \cos \delta^{EW} \cos \delta^T \\
&\quad - 4r_C \cos \delta^{EW} \cos \delta^C] \cos \phi_3 \\
&\quad + 4r_C \cos \delta^C (r_C \cos \delta^C + r_T \cos \delta^T) \cos^2 \phi_3, \quad (25)
\end{aligned}$$

where $\tau^+(\tau^0)$ is a life time of $B^+(B^0)$ and $\tau^+/\tau^0 = 1.086 \pm 0.017$ [30]. We notice that R_1 depends only on r_T , δ^T , and ϕ_3 . If r_T and ϕ_3 can be determined by other observations, R_1 becomes dependent only on δ^T which is the relative strong phase between the effective tree and the effective strong penguin contribution. Subsequently, using the experimental value of R_1 , one can determine the value of δ^T , as shown in the next section.

The direct CP asymmetries are given by

$$\begin{aligned}
\mathcal{A}_{CP}^{0+} &\equiv \frac{\mathcal{B}(B^- \rightarrow \bar{K}^0 \pi^-) - \mathcal{B}(B^+ \rightarrow K^0 \pi^+)}{\mathcal{B}(B^- \rightarrow \bar{K}^0 \pi^-) + \mathcal{B}(B^+ \rightarrow K^0 \pi^+)} \\
&= -2r_A \sin \delta^A \sin \phi_3, \quad (26)
\end{aligned}$$

$$\begin{aligned}
\mathcal{A}_{CP}^{+0} &\equiv \frac{\mathcal{B}(B^- \rightarrow K^- \pi^0) - \mathcal{B}(B^+ \rightarrow K^+ \pi^0)}{\mathcal{B}(B^- \rightarrow K^- \pi^0) + \mathcal{B}(B^+ \rightarrow K^+ \pi^0)} \\
&= -2[r_T \sin \delta^T - r_C \sin \delta^C - r_A \sin \delta^A \\
&\quad + r_T r_{EW} \sin(\delta^T + \delta^{EW}) + r_C r_{EW} \sin(\delta^C + \delta^{EW})] \\
&\quad \times \sin \phi_3 - [2r_T r_C \sin(\delta^T + \delta^C) + r_T^2 \sin 2\delta^T \\
&\quad + r_C^2 \sin 2\delta^C] \sin 2\phi_3, \quad (27)
\end{aligned}$$

$$\begin{aligned}
\mathcal{A}_{CP}^{+-} &\equiv \frac{\mathcal{B}(\bar{B}^0 \rightarrow K^- \pi^+) - \mathcal{B}(B^0 \rightarrow K^+ \pi^-)}{\mathcal{B}(\bar{B}^0 \rightarrow K^- \pi^+) + \mathcal{B}(B^0 \rightarrow K^+ \pi^-)} \\
&= -2r_T \sin \delta^T \sin \phi_3 - r_T^2 \sin 2\delta^T \sin 2\phi_3, \quad (28)
\end{aligned}$$

$$\begin{aligned}
\mathcal{A}_{CP}^{00} &\equiv \frac{\mathcal{B}(\bar{B}^0 \rightarrow \bar{K}^0 \pi^0) - \mathcal{B}(B^0 \rightarrow K^0 \pi^0)}{\mathcal{B}(\bar{B}^0 \rightarrow \bar{K}^0 \pi^0) + \mathcal{B}(B^0 \rightarrow K^0 \pi^0)} \\
&= 2[r_C \sin \delta^C + r_{EW} r_C \sin(\delta^{EW} + \delta^C)] \sin \phi_3 \\
&\quad - r_C^2 \sin 2\delta^C \sin 2\phi_3. \quad (29)
\end{aligned}$$

Notice that considering the conventional hierarchy given in (17) and (18), the direct CP asymmetries \mathcal{A}_{CP}^{+0} (27) and \mathcal{A}_{CP}^{+-} (28) are expected to be almost same including their *signs*, because the dominant contribution to them is identical. However, the current experimental data show that \mathcal{A}_{CP}^{+0} and \mathcal{A}_{CP}^{+-} are quite different from each other and even have the opposite signs to each other, as shown in Table I.

The time-dependent CP asymmetry for $B^0 \rightarrow K_S \pi^0$ is defined as

$$\begin{aligned}
\mathcal{A}_{K_S \pi^0}(t) &\equiv \frac{\Gamma(\bar{B}^0(t) \rightarrow K_S \pi^0) - \Gamma(B^0(t) \rightarrow K_S \pi^0)}{\Gamma(\bar{B}^0(t) \rightarrow K_S \pi^0) + \Gamma(B^0(t) \rightarrow K_S \pi^0)} \\
&\equiv S_{K_S \pi^0} \sin(\Delta m_d t) - C_{K_S \pi^0} \cos(\Delta m_d t), \quad (30)
\end{aligned}$$

where Γ denotes the relevant decay rate and Δm_d is the mass difference between the two B^0 mass eigenstates. The $S_{K_S \pi^0}$ and $C_{K_S \pi^0}$ are CP violating parameters. In the case that the tree contributions are neglected for $B^0 \rightarrow K_S \pi^0$, the mixing-induced CP violating parameter $S_{K_S \pi^0}$ is equal to $\sin(2\phi_1)$ [ϕ_1 ($\equiv \beta$) is the angle of the unitarity triangle].

TABLE I. Experimental data on the CP -averaged branching ratios (\bar{B} in units of 10^{-6}), the direct CP asymmetries (\mathcal{A}_{CP}), and the mixing-induced CP asymmetry ($S_{K_s\pi^0}$) for $B \rightarrow K\pi$ modes. The $S_{K_s\pi^0}$ is equal to $\sin(2\phi_1)$ in the case that tree amplitudes are neglected for $B^0 \rightarrow K_s\pi^0$ [1–13].

	CLEO	Belle	BaBar	Average
$\bar{B}(B^\pm \rightarrow K^0\pi^\pm)$	$18.8^{+3.7+2.1}_{-3.3-1.8}$	$22.0 \pm 1.9 \pm 1.1$	$26.0 \pm 1.3 \pm 1.0$	24.1 ± 1.3
$\bar{B}(B^\pm \rightarrow K^\pm\pi^0)$	$12.9^{+2.4+1.2}_{-2.2-1.1}$	$12.0 \pm 1.3^{+1.3}_{-0.9}$	$12.0 \pm 0.7 \pm 0.6$	12.1 ± 0.8
$\bar{B}(B^0 \rightarrow K^\pm\pi^\mp)$	$18.0^{+2.3+1.2}_{-2.1-0.9}$	$18.5 \pm 1.0 \pm 0.7$	$19.2 \pm 0.6 \pm 0.6$	18.9 ± 0.7
$\bar{B}(B^0 \rightarrow K^0\pi^0)$	$12.8^{+4.0+1.7}_{-3.3-1.4}$	$11.7 \pm 2.3^{+1.2}_{-1.3}$	$11.4 \pm 0.9 \pm 0.6$	11.5 ± 1.0
\mathcal{A}_{CP}^{0+}	$+0.18 \pm 0.24 \pm 0.02$	$+0.05 \pm 0.05 \pm 0.01$	$-0.09 \pm 0.05 \pm 0.01$	-0.02 ± 0.04
\mathcal{A}_{CP}^{+0}	$-0.29 \pm 0.23 \pm 0.02$	$+0.04 \pm 0.04 \pm 0.02$	$+0.06 \pm 0.06 \pm 0.01$	$+0.04 \pm 0.04$
\mathcal{A}_{CP}^{+-}	$-0.04 \pm 0.16 \pm 0.02$	$-0.113 \pm 0.022 \pm 0.008$	$-0.133 \pm 0.030 \pm 0.009$	-0.115 ± 0.018^a
\mathcal{A}_{CP}^{00}	—	$+0.16 \pm 0.29 \pm 0.05$	$-0.06 \pm 0.18 \pm 0.03$	$+0.001 \pm 0.155$
$S_{K_s\pi^0}$	—	$+0.30 \pm 0.59 \pm 0.11$	$+0.35^{+0.30}_{-0.33} \pm 0.04$	$+0.34 \pm 0.29$

^aThis average also includes the CDF result: $-0.04 \pm 0.08 \pm 0.01$.

The expression for $S_{K_s\pi^0}$ (up to r^2 order) is given by

$$\begin{aligned}
S_{K_s\pi^0} = & \sin(2\phi_1)(1 - 2r_C^2\sin^2\phi_3) + \cos(2\phi_1) \\
& \times [2r_C\cos\delta^C\sin\phi_3 + 2r_{EW}r_C\cos(\delta^{EW} + \delta^C) \\
& \times \sin\phi_3 - r_C^2\cos(2\delta^C)\sin(2\phi_3)]. \quad (31)
\end{aligned}$$

The measured value of $S_{K_s\pi^0}$ (Table I) is different from the well-established value of $\sin(2\phi_1) = 0.725 \pm 0.037$ measured through $B \rightarrow J/\psi K^{(*)}$ [1]. It may indicate that the subleading terms including r_C and r_{EW} in Eq. (31) play an important role.

III. THE $B \rightarrow K\pi$ PUZZLE AND ITS IMPLICATION

We first summarize the present status of the experimental results on $B \rightarrow K\pi$ modes in Table I, which includes the BRs, the direct CP asymmetries (\mathcal{A}_{CP}), and the mixing-induced CP asymmetry ($S_{K_s\pi^0}$). We see that the averages of the current experimental values for the BRs include only a few percent errors. Furthermore, the direct CP asymmetry in $B^0 \rightarrow K^\pm\pi^\mp$ has been recently observed by the BaBar and Belle collaborations whose values are in good agreement with each other (Table I): the world average value is

$$\mathcal{A}_{CP}^{+-} = -0.115 \pm 0.018. \quad (32)$$

The direct CP asymmetry data for the other $B \rightarrow K\pi$ modes involve large uncertainties. We also present the values of R_1 , R_c , and R_n , defined in Eqs. (23)–(25), which are obtained from the experimental results given in Table I:

$$R_1 = 0.82 \pm 0.06, \quad (33)$$

$$R_c = 1.00 \pm 0.09, \quad (34)$$

$$R_n = 0.82 \pm 0.08. \quad (35)$$

It has been also claimed that within the SM, $R_c - R_n \approx 0$ [16,31]. From Eqs. (24) and (25), it is indeed clear that

$R_c \approx R_n$, if the r^2 order terms including r_{EW} or r_C are negligible. In other words, any difference between R_c and R_n would arise from the contributions from the subdominant r^2 order terms including r_{EW} or r_C . The above experimental data show the pattern $R_c > R_n$ [16,31], which would imply the enhancement of the EW penguin and/or the color-suppressed tree contributions. We will investigate the implication of the data below.

We remind that assuming the conventional hierarchy as in Eqs. (17) and (18), \mathcal{A}_{CP}^{+0} is expected to be almost the same as \mathcal{A}_{CP}^{+-} ; in particular, they would have the *same* sign. However, the data show that \mathcal{A}_{CP}^{+0} differs by 3.5σ from \mathcal{A}_{CP}^{+-} . This is a very interesting observation with the new measurements of \mathcal{A}_{CP}^{+-} by BaBar and Belle, even though the measurements of \mathcal{A}_{CP}^{+0} still include sizable errors. One may need to explain on the theoretical basis how this feature can happen.

Based on the current experimental data shown in Table I, we critically investigate their implications to the underlying theory on the $B \rightarrow K\pi$ processes. There are nine observables available for the $B \rightarrow K\pi$ modes as shown in Table I, but if the expectedly very small annihilation term r_A is neglected, the observable \mathcal{A}_{CP}^{0+} becomes irrelevant and only eight observables remain relevant. There are also eight parameters ($|P|$, r_T , r_{EW} , r_C , δ^T , δ^{EW} , δ^C , ϕ_3) relevant to the above observables, neglecting the very small terms including r_A and r_{EW}^C [see Eqs. (19)–(29) (29)]. In our numerical analysis, we take into account the above eight parameters. [Equivalently, we can use only seven observables (*i.e.*, three R_i ($i = 1, c, n$) and the CP asymmetries in Table I), and take into account the seven parameters (except for $|P|$ among the above eight parameters).]

We remind that among the data shown in Table I, five of them, such as the BRs and \mathcal{A}_{CP}^{+-} , involve relatively small uncertainties, but the others still include large errors. Based on this observation, we consider four different cases as follows. (i) We first use only the four BRs in our analysis. (ii) Then, the data for \mathcal{A}_{CP}^{+-} are also considered in addition

to the BRs. Since the observables used in the cases (i) and (ii) are measured relatively accurately, the result from these cases would provide more solid implications. (iii) Then, we also use the data for $S_{K_s\pi^0}$ besides those used in the case (ii). (iv) Finally we use all the currently available data.

In Fig. 1, we show the excluded region for r_C and r_{EW} by the current data for the cases (i)–(iv). The graph has been obtained by using the current data given in Table I] as constraints and directly solving Eqs. (19)–(22), (27)–(29) and (31) for $54^\circ \leq \phi_3 \leq 67^\circ$ and $0 \leq r_T \leq 0.4$. [Here we use the value of ϕ_3 given by the unitarity triangle fit [32]. In order to study the effect of r_T to the result, we vary the value of r_T from 0 to 0.4.] The bold straight (parallel and vertical) lines denote the conventional values of $r_C \approx 0.02$ and $r_{EW} \approx 0.14$, respectively. The solid, dotted, dashed, dot-dashed lines, respectively, correspond to each case of (i)–(iv) in order: *i.e.*, each case of using (i) only 4 BRs, (ii) 4BRs + \mathcal{A}_{CP}^{+-} , (iii) 4BRs + \mathcal{A}_{CP}^{+-} + $S_{K_s\pi^0}$, and (iv) all the available data.

One should keep in mind that in the cases (i)–(iii) only the “excluded” regions for r_C and r_{EW} are meaningful at 1σ level in Fig. 1, because in these cases the number of parameters are larger than that of the relevant equations so that the other regions (except for the excluded regions) do not exactly mean the “allowed” regions for r_C and r_{EW} at 1σ level.

The result shows that when the data only for the BRs of $B \rightarrow K\pi$ modes are taken into account [solid line; case (i)], the conventional SM predictions of both $r_{EW} \approx 0.14$ and

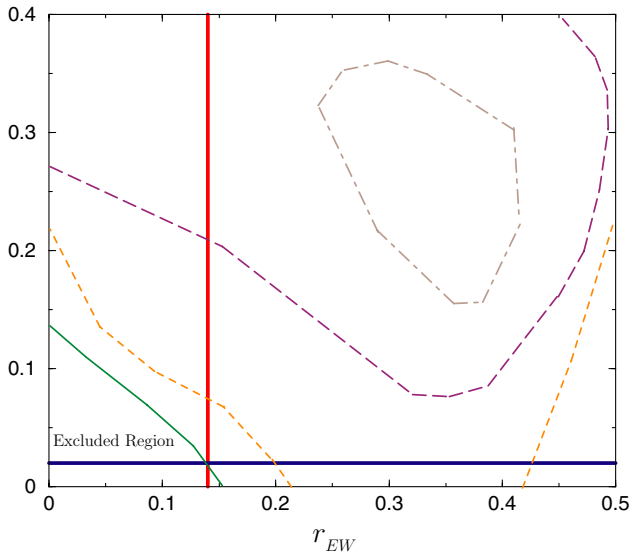


FIG. 1 (color online). The excluded region for r_C and r_{EW} . The bold straight (parallel and vertical) lines denote the conventional values of $r_C \approx 0.02$ and $r_{EW} \approx 0.14$, respectively. The solid, dotted, dashed, dot-dashed lines, respectively, correspond to the case of using only 4 BRs, 4BRs + \mathcal{A}_{CP}^{+-} , 4BRs + \mathcal{A}_{CP}^{+-} + $S_{K_s\pi^0}$, and all the available data. Here $54^\circ \leq \phi_3 \leq 67^\circ$ and $0 \leq r_T \leq 0.4$ were used.

$r_C \approx 0.02$ are not completely excluded by the data. But, we should add a remark that this fact holds only for $r_T \approx 0.4$ (which is larger than the conventional SM estimate of $r_T \approx 0.2$), because for smaller r_T larger values of r_{EW} and r_C are excluded: *e.g.*, for $r_T = 0.3$ or smaller, $r_{EW} \approx 0.14$ together with $r_C \approx 0.02$ is no more allowed. In other words, for the conventional value of $r_T \approx 0.2$, the data for the BRs indicates that the EW penguin and/or the color-suppressed tree term need(s) to be enhanced. [This conclusion equivalently holds when the data only for R_i ($i = 1, c, n$) given in Eqs. (33)–(35) are considered.]

When the constraint from the measured A_{CP}^{+-} is added to the case (i), the conventional values of r_{EW} and r_C are not allowed at the same time (dotted line). For instance, if $r_{EW} \approx 0.14$, then the values of r_C smaller than 0.07 are excluded. On the other hand, if $r_C \approx 0.02$, then the values of r_{EW} smaller than 0.19 are not allowed by the data. It would be also possible that both r_{EW} and r_C are simultaneously enhanced: *e.g.*, $r_{EW} \approx 0.17$ and $r_C \approx 0.05$ are not excluded in this case (ii). Thus, we see that even in this conservative case of considering only 5 (relatively precisely measured) observables, the data strongly indicate a sizable enhancement of the EW penguin term r_{EW} or the color-suppressed tree term r_C , or both of them.

The dashed line shows the result for the case of adding one more constraint from $S_{K_s\pi^0}$ to the case (ii). It is interesting to note that the values of r_C smaller than 0.08 are completely excluded in this case (iii), independent of values of r_{EW} .

Finally we consider all the available data for $B \rightarrow K\pi$ modes shown in Table I. In this case, the number of parameters are the same as that of the relevant equations so that one can determine the allowed values of the parameters by solving the equations numerically. In order to find the allowed region for the parameters, when combining all the data, we carefully regulate the errors in the data to be within 1σ in total. The result is represented as the dot-dashed line [case (iv)]. The allowed values for r_{EW} and r_C are limited to a rather small region at 1σ level: roughly, $0.24 \leq r_{EW} \leq 0.41$ and $0.16 \leq r_C \leq 0.36$. Notice that *simultaneous* enhancements of r_C and r_{EW} are indicated in this case. In order to confirm this result in a statistically more reliable way, we shall use the χ^2 minimization technique in the next section.

In Fig. 2, we present R_1 and A_{CP}^{+-} as a function of δ^T . We remind that both R_1 and A_{CP}^{+-} depend only on r_T , δ^T and ϕ_3 . The left one of the figure shows R_1 as a function of δ^T for $\phi_3 = 40^\circ, 60^\circ, 80^\circ$, respectively, where r_T is fixed as 0.2. The allowed regions are $\delta^T \leq 40^\circ$ or $\delta^T \geq 320^\circ$. The possibility of the vanishing δ^T is not excluded in this case. In the right one of the figure, A_{CP}^{+-} versus δ^T is presented for $r_T = 0.2$ and $\phi_3 = 40^\circ, 60^\circ, 80^\circ$, respectively. Combining the results from the left and right ones, we find that the possibility of a large δ^T is ruled out and the favored value of δ^T is nonzero and in between 20° and 30° for $r_T = 0.2$ and $40^\circ \leq \phi_3 \leq 80^\circ$ [14,24].

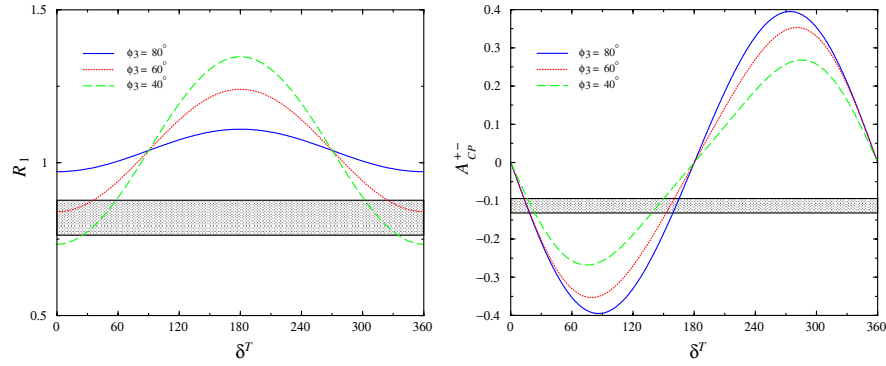


FIG. 2 (color online). R_1 and A_{CP}^{+-} as a function of δ^T for three different values of $\phi_3 = 40^\circ, 60^\circ, 80^\circ$, respectively. The shaded regions denote the experimental limits.

IV. THE χ^2 ANALYSIS USING $B \rightarrow K\pi$ DECAYS

In the numerical analysis, we use 8 observables, as shown in Table I (except \mathcal{A}_{CP}^{0+} which becomes irrelevant if r_A is neglected).

Case (a): In this case, we have eight observables as above and seven parameters ($|\tilde{P}|, r_T, r_{EW}, r_C, \delta^T, \delta^{EW}, \delta^C$) so that the degrees of freedom (*d.o.f.*) for the fit is 1. The parameter values for the best fit are presented in Table II for three different values of ϕ_3 chosen from the unitarity triangle fit: $\phi_3 = 54^\circ, 60^\circ$, or 67° . The minimum values of χ^2 (χ_{\min}^2) in each case are also shown in the table.

For instance, in the case of $\phi_3 = 60^\circ$, we find the best fit with $\chi_{\min}^2/d.o.f. = 0.005$. The corresponding parameters are

$$|\tilde{P}| = 1.23 \times 10^{-6} \text{ GeV}, \quad r_T = 0.25, \quad (36)$$

$$r_{EW} = 0.37, \quad r_C = 0.25,$$

$$\delta^T = 13.0^\circ, \quad \delta^{EW} = 260.4^\circ, \quad \delta^C = 197.8^\circ. \quad (37)$$

Using these parameter values, the observables are predicted as

$$\bar{B}^{0+} = 24.08 \times 10^{-6}, \quad \bar{B}^{+0} = 12.10 \times 10^{-6}, \quad (38)$$

$$\bar{B}^{+-} = 18.21 \times 10^{-6}, \quad \bar{B}^{00} = 11.51 \times 10^{-6}, \quad (39)$$

$$\mathcal{A}_{CP}^{+0} = +0.04, \quad \mathcal{A}_{CP}^{+-} = -0.119, \quad (40)$$

$$\mathcal{A}_{CP}^{00} = -0.007, \quad S_{K_s\pi^0} = +0.33,$$

which are in good agreement with the central values of all the data.

We see that in this case the best fit value of the color-suppressed tree contribution r_C is comparable to that of the color-allowed tree contribution r_T , and the best fit value of the EW penguin contribution r_{EW} is also about 2.6 times larger than the conventionally estimated one. Table II shows that as ϕ_3 increase from 54° to 67° , the best fit values of r_T, r_{EW} and r_C also increases from 0.20, 0.35 and 0.25 to 0.34, 0.40 and 0.27, respectively. The best fit indicates that in comparison to the conventional estimates within the SM, the color-suppressed tree contribution should be enhanced by more than an order of magnitude, and the EW penguin contribution needs to be enhanced up to a factor of 3.

In Fig. 3, the allowed values of r_{EW} and r_C are presented. The “x” marks denote the best fit values together with the corresponding values of $r_T = 0.20, 0.25, 0.34$ for $\phi_3 = 54^\circ, 60^\circ, 67^\circ$, respectively. The regions surrounded by the solid, the dotted, and the dashed lines represent the allowed values of r_{EW} and r_C at 1σ level for $\phi_3 = 54^\circ, 60^\circ, 67^\circ$, respectively. It is obvious that the smallest allowed value of r_C at 1σ level is at least 7 times larger than the conventional value (≈ 0.02), and the allowed value of r_{EW} is also larger than its conventional SM estimate (≈ 0.14): $r_{EW} > 0.21$ for $54^\circ \leq \phi_3 \leq 67^\circ$. Therefore, the current experimental results for $B \rightarrow K\pi$ decays strongly imply (large) enhancements of both the EW penguin and the color-suppressed tree contributions.

Case (b): Now we use all the eight parameters including ϕ_3 together with the same eight observables as before. In this case, the ϕ_3 varies from 54° to 67° , which are chosen from the unitarity triangle fit. The result at 1σ level is shown in Fig. 4. We note that this result confirms that of the case (iv) (the dot-dashed line) shown in Fig. 1. The best fit

TABLE II. The theoretical parameter values for the best fit in Case (a).

ϕ_3	$ P $ (in 10^{-6} GeV)	r_T	r_{EW}	r_C	δ^T	δ^{EW}	δ^C	$\chi_{\min}^2/d.o.f.$
54°	1.23	0.20	0.35	0.25	17.9°	254.9°	195.1°	0.01
60°	1.23	0.25	0.37	0.25	13.0°	260.4°	197.8°	0.005
67°	1.22	0.34	0.40	0.27	8.6°	256.6°	202.2°	0.45

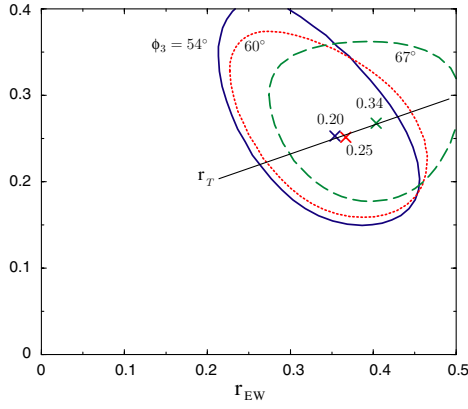


FIG. 3 (color online). Case (a): the allowed values of r_{EW} and r_C by the current data for $B \rightarrow K\pi$. The x marks denote the best fit values together with the corresponding values of r_T for $\phi_3 = 54^\circ, 60^\circ, 67^\circ$, respectively. The regions surrounded by the solid, the dotted, and the dashed lines represent the allowed values of r_{EW} and r_C at 1σ level for $\phi_3 = 54^\circ, 60^\circ, 67^\circ$, respectively.

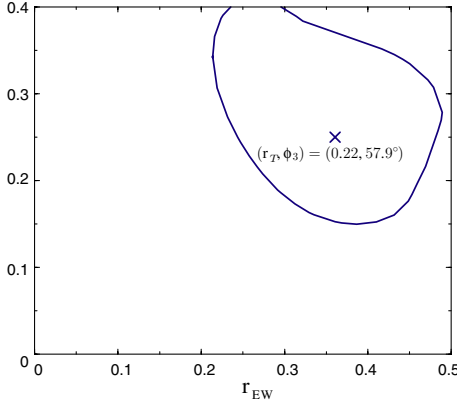


FIG. 4 (color online). Case (b): the allowed values of r_{EW} and r_C by the current data for $B \rightarrow K\pi$. Here all the eight parameters, including ϕ_3 , are varied. The x mark denotes the best fit value where $r_T = 0.22$ and $\phi_3 = 57.9^\circ$.

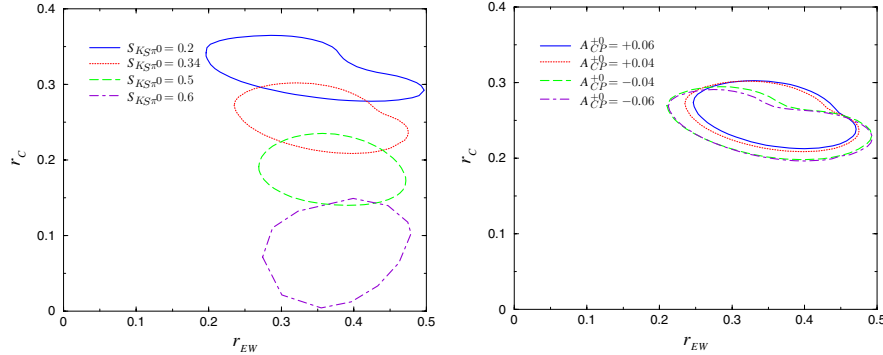


FIG. 5 (color online). Illustration of the allowed values of r_{EW} and r_C at 1σ level by the current data for $B \rightarrow K\pi$, for a given $S_{K_s\pi^0}$ (left figure) or A_{CP}^{+0} (right figure). In the left figure, $S_{K_s\pi^0}$ is assumed to be 0.20, 0.34, 0.50, 0.60, respectively, (plus 20% error in each case). In the right one, A_{CP}^{+0} is assumed to be $\pm 0.040, \pm 0.060$, respectively, (plus 20% error in each case).

values are

$$|\tilde{P}| = 1.23 \times 10^{-6} \text{ GeV}, \quad r_T = 0.22, \quad (41)$$

$$r_{EW} = 0.36, \quad r_C = 0.25,$$

$$\begin{aligned} \delta^T &= 14.8^\circ, & \delta^{EW} &= 258.5^\circ, \\ \delta^C &= 196.7^\circ, & \phi_3 &= 57.9^\circ. \end{aligned} \quad (42)$$

The conclusion claimed in the case (a) holds in this case as well. That is, the present experimental results for $B \rightarrow K\pi$ decays strongly indicate simultaneous (large) enhancements of the EW penguin and the color-suppressed tree contributions.

Finally we would like to make a comment on sensitivity between the parameter r_C and the observable $S_{K_s\pi^0}$. As implied in Eq. (31), the theoretical prediction of $S_{K_s\pi^0}$ can be sensitive to the parameter r_C . For illustration, in the left one of Fig. 5, we show the allowed values of r_{EW} and r_C at 1σ level by the current data for $B \rightarrow K\pi$, when the value of $S_{K_s\pi^0}$ changes, keeping the values of the other observables fixed as in Table I. We first vary $S_{K_s\pi^0}$ around the present experimental value: specifically, $S_{K_s\pi^0}$ is assumed to be $(0.20 \pm 0.04), (0.34 \pm 0.068), (0.50 \pm 0.10), (0.60 \pm 0.12)$, respectively. Here just for the illustrative purpose, we set 20% errors in each case. (Also, to be consistent, we set 20% errors to all the data whose current errors are larger than 20%, such as A_{CP}^{ij} .) It is clear that as $S_{K_s\pi^0}$ varies, the allowed region for r_C varies sensitively: as $S_{K_s\pi^0}$ increases, the allowed value of r_C decreases. In contrast, r_{EW} is not sensitive to the change of $S_{K_s\pi^0}$. Just for comparison, in the right one of Fig. 5, we also present the case that the value of A_{CP}^{+0} changes, keeping the values of the other ones fixed as in Table I. Again for the illustrative purpose, A_{CP}^{+0} is assumed to be $(+0.040(-0.040) \pm 0.008), (0.060(-0.060) \pm 0.012)$, respectively. (To be consistent, we also set 20% errors to all the data whose current errors are larger than 20%, such as $S_{K_s\pi^0}$ and A_{CP}^{ij} .) In contrast to

the case of the left figure, both r_{EW} and r_C are insensitive to the change of A_{CP}^{+0} .

V. CONCLUSION

We have studied the decay processes $B \rightarrow K\pi$ in a phenomenological way. Using the currently available experimental data for all the $B \rightarrow K\pi$ modes, we have determined the allowed values of the relevant theoretical parameters, such as $|\tilde{P}|$, r_T , r_{EW} , r_C , δ^T , δ^{EW} , δ^C , ϕ_3 . In order to find the most likely values of the parameters in a statically reliable way, we used the χ^2 analysis.

Our result shows that the current data for $B \rightarrow K\pi$ decays strongly indicate (large) enhancements of both the EW penguin and the color-suppressed tree contributions: *e.g.*, roughly, $0.21 \leq r_{EW} \leq 0.49$ and $0.15 \leq r_C \leq 0.43$ at 1σ level. The best fit values are $r_{EW} = 0.36$ and $r_C = 0.25$. The favored values of r_{EW} and r_C are larger than the SM estimates ($r_{EW} \approx 0.14$ and $r_C \approx 0.02$) by about a factor of 2.5 and 12, respectively.

It should be noted that in the case of using only the BRs (*i.e.*, not including CP asymmetries), the conventional values of r_{EW} and r_C may not be completely excluded, if the large value of r_T (*e.g.*, $r_T \approx 0.4$) is assumed.

ACKNOWLEDGMENTS

The work of C. S. K. was supported by in part by the Korea Research Foundation Grant funded by the Korean Government (MOEHRD) No. KRF-2005-070-C00030. C. S. K. also received support from JSPS. The work of S. O. was supported by Korea Research Foundation Grant (KRF-2004-050-C00005). The work of C. Y. was supported in part by Brain Korea 21 Program and in part by Grant No. F01-2004-000-10292-0 of KOSEF-NSFC International Collaborative Research Grant and in part by the Korea Research Foundation Grant funded by the Korean Government (MOEHRD) No. R02-2003-000-10050-0.

-
- [1] Heavy Flavor Averaging Group, <http://www.slac.stanford.edu/xorg/hfag/>.
- [2] A. Bornheim *et al.* (CLEO Collaboration), Phys. Rev. D **68**, 052002 (2003).
- [3] Y. Chao *et al.* (Belle Collaboration), Phys. Rev. D **69**, 111102 (2004).
- [4] B. Aubert *et al.* (BABAR Collaboration), Phys. Rev. Lett. **89**, 281802 (2002).
- [5] B. Aubert *et al.* (BABAR Collaboration), hep-ex/0408062.
- [6] B. Aubert *et al.* (BABAR Collaboration), hep-ex/0408080.
- [7] B. Aubert *et al.* (BABAR Collaboration), hep-ex/0408081.
- [8] K. Abe, *XXII International Symposium on Lepton-Photon Interactions at High Energy, Uppsala, Sweden, 2005* (unpublished).
- [9] S. Chen *et al.* (CLEO Collaboration), Phys. Rev. Lett. **85**, 525 (2000).
- [10] B. Aubert *et al.* (BaBar Collaboration), Phys. Rev. Lett. **93**, 131801 (2004).
- [11] Y. Chao *et al.* (BELLE Collaboration), Phys. Rev. D **71**, 031502 (2005).
- [12] Y. Chao *et al.* (Belle Collaboration), Phys. Rev. Lett. **93**, 191802 (2004).
- [13] K. Abe *et al.* (BELLE Collaboration), hep-ex/0409049.
- [14] S. Mishima and T. Yoshikawa, Phys. Rev. D **70**, 094024 (2004).
- [15] Y. L. Wu and Y. F. Zhou, Phys. Rev. D **71**, 021701 (2005); Phys. Rev. D **72**, 034037 (2005).
- [16] A. J. Buras, R. Fleischer, S. Recksiegel, and F. Schwab, Acta Phys. Pol. B **36**, 2015 (2005); hep-ph/0411373.
- [17] Y. Y. Charm and H. n. Li, Phys. Rev. D **71**, 014036 (2005).
- [18] X. G. He and B. H. J. McKellar, hep-ph/0410098.
- [19] S. Baek, P. Hamel, D. London, A. Datta, and D. A. Suprun, Phys. Rev. D **71**, 057502 (2005).
- [20] T. Carruthers and B. H. J. McKellar, hep-ph/0412202.
- [21] S. Nandi and A. Kundu, hep-ph/0407061.
- [22] T. Morozumi, Z. H. Xiong, and T. Yoshikawa, hep-ph/0408297; X. Q. Li and Y. D. Yang, hep-ph/0508079
- [23] M. Gronau, O. F. Hernandez, D. London, and J. L. Rosner, Phys. Rev. D **50**, 4529 (1994); M. Gronau, J. L. Rosner, and D. London, Phys. Rev. Lett. **73**, 21 (1994); O. F. Hernandez, D. London, M. Gronau, and J. L. Rosner, Phys. Lett. B **333**, 500 (1994); M. Gronau, O. F. Hernandez, D. London, and J. L. Rosner, Phys. Rev. D **52**, 6374 (1995); C. S. Kim, D. London, and T. Yoshikawa, Phys. Rev. D **57**, 4010 (1998).
- [24] T. Yoshikawa, Phys. Rev. D **68**, 054023 (2003).
- [25] Y. Y. Keum, H. N. Li, and A. I. Sanda, Phys. Rev. D **63**, 054008 (2001); Phys. Lett. B **504**, 6 (2001); AIP Conf. Proc. **618**, 229 (2002).
- [26] M. Neubert and J. L. Rosner, Phys. Rev. Lett. **81**, 5076 (1998).
- [27] H. Y. Cheng, C. K. Chua, and A. Soni, Phys. Rev. D **71**, 014030 (2005).
- [28] C. S. Kim, S. Oh, and C. Yu, Phys. Lett. B **621**, 259 (2005).
- [29] Y. Y. Keum, T. Kurimoto, H. N. Li, C. D. Lu, and A. I. Sanda, Phys. Rev. D **69**, 094018 (2004).
- [30] S. Eidelman *et al.* (Particle Data Group), Phys. Lett. B **592**, 1 (2004).
- [31] A. J. Buras, R. Fleischer, S. Recksiegel, and F. Schwab, Phys. Rev. Lett. **92**, 101804 (2004); Nucl. Phys. **B697**, 133 (2004).
- [32] M. Bona *et al.* (UTfit Collaboration), J. High Energy Phys. **07** (2005) 028.